molecules

MDPI

Article

Isohexide-Based Tunable Chiral Platforms as Amide- and Thiourea-Chiral Solvating Agents for the NMR Enantiodiscrimination of Derivatized Amino Acids

Federica Cefalì, Anna Iuliano *, Federica Balzano *, Gloria Uccello Barretta, Valerio Zullo and Carlo Baldassari

Department of Chemistry and Industrial Chemistry, University of Pisa, Via G. Moruzzi 13, 56124 Pisa, Italy; f.cefali@studenti.unipi.it (F.C.); gloria.uccello.barretta@unipi.it (G.U.B.); valeriozullo@hotmail.it (V.Z.); c.baldassari@studenti.unipi.it (C.B.)

* Correspondence: anna.iuliano@unipi.it (A.I.); federica.balzano@unipi.it (F.B.)

Abstract: New arylamide- and arylthiourea-based chiral solvating agents (CSAs) were synthesized starting from commercially available isomannide and isosorbide. The two natural isohexides were transformed into the three amino derivatives, having isomannide, isosorbide, and isoidide stereochemistry, then the amino groups were derivatized with 3,5-dimethoxybenzoyl chloride or 3,5-bis(trifluoromethyl)phenyl isothiocyanate to obtain the CSAs. Bis-thiourea derivative containing the 3,5-bis(trifluoromethyl)phenyl moiety with exo–exo stereochemistry was remarkably efficient in the differentiation of NMR signals (NH and acetyl) of enantiomers of *N*-acetyl (*N*-Ac) amino acids in the presence of 1,4-diazabicyclo[2,2,2]octane (DABCO). Nonequivalences in the ranges of 0.104–0.343 ppm and 0.042–0.107 ppm for NH and acetyl groups, respectively, allowed for very accurate enantiomeric excess determination, and a reliable correlation was found between the relative positions of signals of enantiomers and their absolute configuration. Therefore, a complete stereochemical characterization could be performed. Dipolar interactions detected in the ternary mixture CSA/*N*-Ac-valine/DABCO led to the identification of a different interaction model for the two enantiomers, involving the formation of a one-to-one substrate/CSA complex for (*S*)-*N*-Ac-valine and a one-to-two complex for (*R*)-*N*-Ac-valine, as suggested by the complexation stoichiometry.

Keywords: absolute configuration; chiral auxiliary; enantiomeric purity; chiral pool; NMR spectroscopy

check for updates

Citation: Cefalì, F.; Iuliano, A.; Balzano, F.; Uccello Barretta, G.; Zullo, V.; Baldassari, C. Isohexide-Based Tunable Chiral Platforms as Amide- and Thiourea-Chiral Solvating Agents for the NMR Enantiodiscrimination of Derivatized Amino Acids. *Molecules* **2024**, *29*, 1307. https://doi.org/10.3390/molecules29061307

Academic Editor: Paride Papadia

Received: 21 February 2024
Revised: 8 March 2024
Accepted: 11 March 2024
Published: 15 March 2024

Copyright: © 2024 by the authors. Licensee MDPI, Basel, Switzerland. This article is an open access article distributed under the terms and conditions of the Creative Commons Attribution (CC BY) license (https://creativecommons.org/licenses/by/4.0/).

1. Introduction

The growing awareness of the impact of chirality on human life has prompted the research towards accurate, reproducible, and, if possible, direct methods for the determination of the enantiomeric purity of chiral compounds.

Over the years, chromatographic [1–5] and spectroscopic/spectrometric [6–13] methods have been developed and, among the latter, NMR spectroscopy has emerged as one of the most versatile investigation techniques. Beyond its analytical potentialities, the supremacy of NMR spectroscopy is also due to the possibility of easy investigation of the discrimination processes at a molecular level.

NMR methods of enantiodifferentiation are based on the use of chiral auxiliaries to convert the enantiomers into intrinsically anisochronous diastereomers. Chiral auxiliaries for NMR spectroscopy can be grouped in three classes, based on the nature of the interactions stabilizing the diastereomers: chiral solvating agents (CSAs) [11,12], chiral derivatizing agents (CDAs) [12], and chiral lanthanide shift agents (CLSRs) [12]. The first class emerged for ease of use. CSAs commonly interact with the enantiomeric substrates by means of non-covalent interactions, such as dipole–dipole, π–π and hydrogen bond formation, giving rise to couples of transient diastereomers. A notable exception is represented by chiral liquid

crystals (CLCs), which offer unprecedented versatility due to the fact that the substrate does not require any specific, directed interaction with the liquid crystal. Consequently, CLCs have the potential to differentiate a wide range of chiral molecules, encompassing organic and inorganic compounds, as well as metal complexes. One peculiarity of CLCs is their capability to differentiate nuclei that are remote from the chiral center, which presents a challenge for the majority of CSAs [13,14].

For the enantiodifferentiation of chiral substrates by any other kind of CSAs, hydrogen bond formation is mandatory for the achievement of the transient diastereomers. Therefore, CSAs endowed with amide and especially thiourea functions should be privileged due to the enhanced acidity and hence hydrogen bond-donating capabilities of these moieties. These functionalities can be easily embedded in chiral platforms by using simple synthetic procedures, which entail the reaction of a chiral amine or diamine with acyl chlorides or isothiocyanates [15,16].

Chiral diamine obtained from precursors belonging to chiral pool can represent an attractive choice for the synthesis of bis-amide and bis-thiourea CSAs, as their natural precursors are readily available in enantiomerically pure forms.

Isohexides, namely isomannide (**1**, Figure 1) and isosorbide (**2**, Figure 1), which are chiral compounds coming from the chiral pool and endowed with interesting proprieties (cheap, non-toxic and obtained from renewable resources) [17–19], and also isoidide (**3**, Figure 1), which can be obtained from isomannide, possess structural features making them good candidates for use as chiral scaffolds for the preparation of chiral auxiliaries for enantioselective processes [20–23]. Their vaulted structure, endowed with two hydroxyl groups characterized by different relative stereochemistry in different isohexides, allows the creation of U-, N- or W-shaped derivatives (Figure 1) showing interesting enantiorecognition features dependent not only on the nature of the derivatizing moieties but also on the stereochemistry of the final compounds.

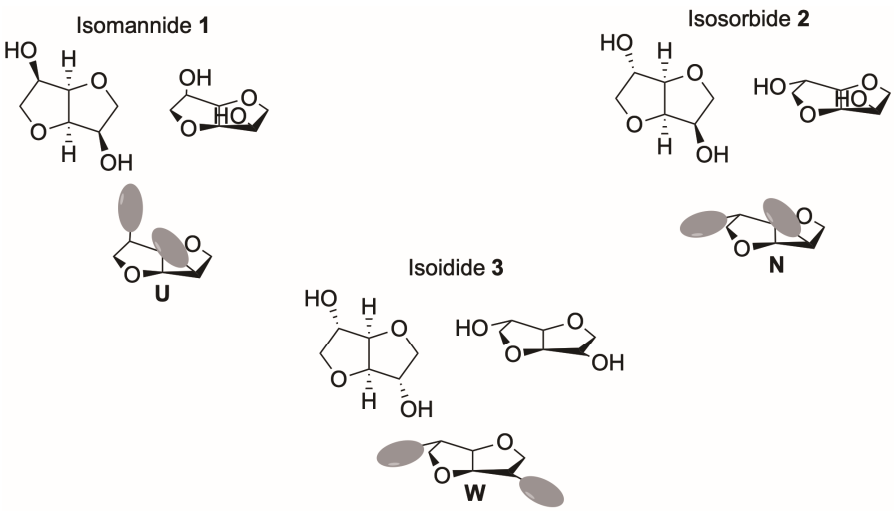

Figure 1. Structures of isohexides and their derivatives.

Ionic liquids derived from U-shaped isomannide behaved as chiral tweezers [23], whereas N-shaped aryl carbamates of isosorbide were successfully used as CSAs for the determination of the enantiomeric composition of amino acid derivatives [22] (Scheme 1, left panel). Those results clearly showed that tuning of the structural features allowed well performing CSAs to be obtained and that the presence of two aryl moieties on the isohexide scaffold was mandatory to achieve good enantiodiscrimination.

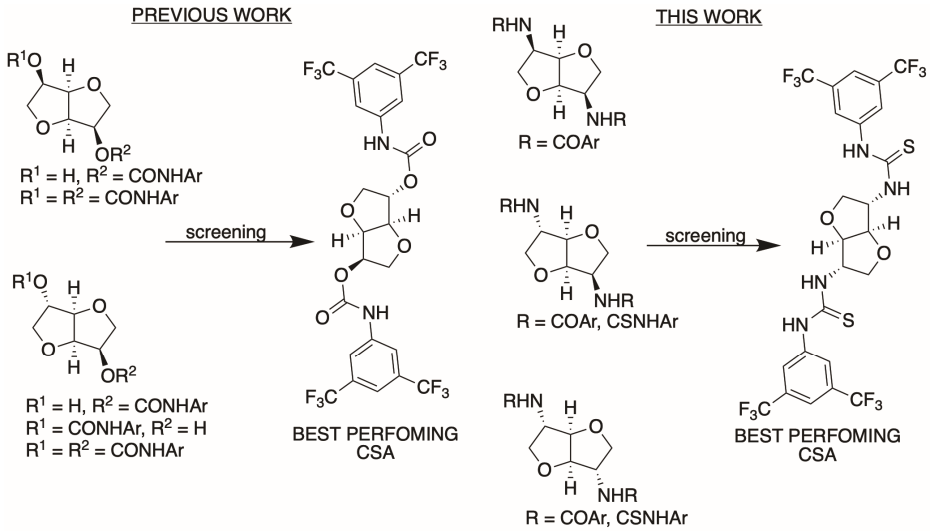

Scheme 1. Use of isohexide derivatives as CSAs.

Starting from these previously reported results, as a part of our ongoing research into the preparation of new, simple, biobased, and efficient CSAs for NMR applications, we turned our attention to the use of amino-derived compounds, such as arylamides or arylthioureas (Scheme 1, right panel). This choice was made while also considering that U-, N-, or W-shaped amino derivatives of isohexides can be easily obtained when starting from commercially available isomannide and isosorbide through stereo-controlled interconversion of the hydroxyl groups to amino groups, followed by the introduction of aryl moieties by amide or thiourea bond formation.

Chiral amides [24–29] and especially chiral arylthioureas [30–38] are known to exhibit excellent enantiodiscriminating capabilities when employed as CSAs for the NMR enantiodiscrimination of chiral carboxylic acids [30–35] and derivatives of amino acids [35–38].

Herein, we report the synthesis of U-, N- and W-shaped isohexide derived arylamides (Scheme 1) and preliminary screening aimed at finding the most suitable structures for NMR enantiodiscrimination, with the synthesis of arylthioureas having the selected structures, followed by additional fast screening to identify the best performing CSA. The W-shaped arylthiourea molecule emerged as the best performing CSA, and this was finally tested in the enantiodiscrimination of amides of different amino acids under optimized analysis conditions. A complete characterization of the best performing CSA together with the study of the enantiodiscrimination mechanism is also presented.

2. Results and Discussion

The synthesis of the amino derivatives of the three isohexides was carried out as described in Scheme 2, starting from commercially available isosorbide and isomannide and from isoidide, which was obtained by Mitsunobu reaction on isomannide with benzoic acid, followed by hydrolysis of the benzoate groups [39].

As reported in Scheme 2, the first step of the synthetic route was the conversion of isohexides **1**–**3** into the corresponding ditriflates. The derivatization was performed by reacting the starting diols **1**–**3** with trifluoromethanesulfonic anhydride in the presence of pyridine at 0 °C. The chemically pure **4** products were obtained in good yields (around 90%), after simple aqueous work-up. Compounds **4** were then converted into diazides **5** via nucleophilic displacement of the triflate groups by sodium azide. As has been well established, the reaction follows a S_{N2} mechanism, thus leading to a complete inversion of configuration at the stereogenic centers bearing the functional groups. As a result, the isomannide-like azide was obtained from the isoidide triflate, and the isomannide triflate was converted into isoidide-like azide, whereas the stereochemistry of the isosorbide core remained unaltered. The reaction was carried out with a high excess of sodium azide in DMF as the solvent at RT, to boost the process toward nucleophilic displacement while

minimizing as much as possible the competitive elimination reaction. However, even using these reaction conditions, the formation of the elimination side product was observed, as already reported [39,40]. The extent of the formation of this product strongly depended on the stereochemistry of the triflate. It was observed that when the nucleophile approached from the less hindered convex side of the isohexide, as in the case of endo-triflate, the elimination side reaction did not take place at all, but when the nucleophile approached from the more hindered concave side, as for the exo-triflate, the formation of at least a 30% proportion of elimination product was observed. For this reason, only diazide **5a**, having two exo-azido groups, was obtained as a chemically pure product after aqueous work-up, whereas the other diazides required chromatographic purification. The reaction was totally stereospecific with all substrates, as confirmed by the analysis of the NMR spectra of the three diazides, which showed the presence of only one set of signals for each nucleus in **5b** or for each couple of equivalent nuclei in **5a** and **5c**, so confirming that no epimerization occurred at the stereogenic centers. The diazides were eventually reduced to the corresponding diamines, in good yields, by catalytic hydrogenation.

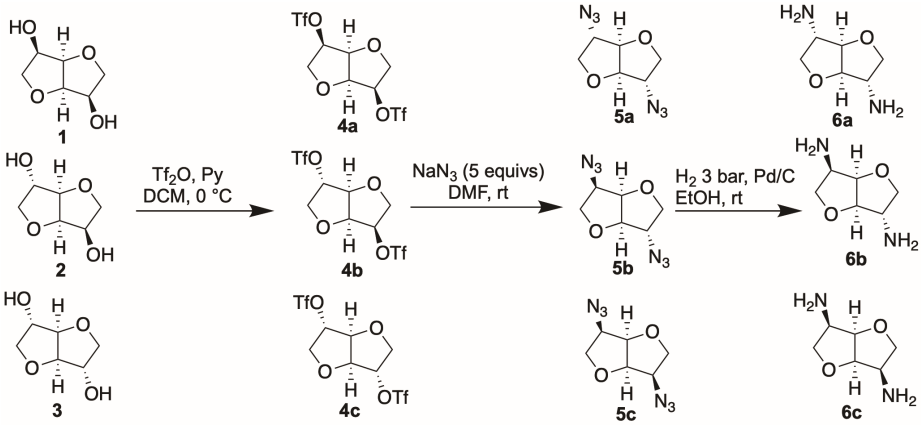

Scheme 2. Synthesis of amino derivatives of isohexides **6**.

The amino derivatives of isohexides were then converted to arylamides and arylthioureas by reacting diamines **6** with 3,5-dimethoxybenzoyl chloride and 3,5-bis (trifluoromethyl)phenyl isothiocyanate, respectively, under standard reaction conditions (Scheme 3).

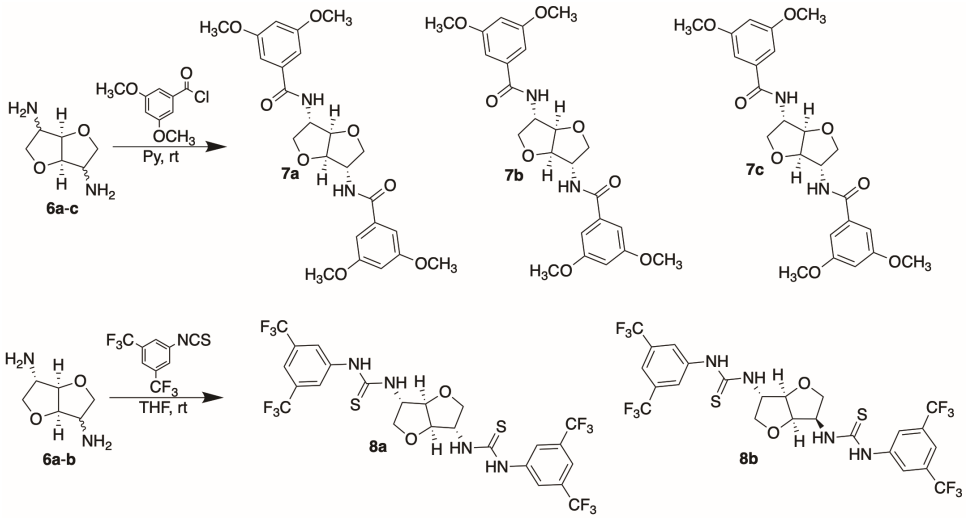

Scheme 3. Synthesis of bis-amides **7** and bis–thioureas **8**.

The enantiodiscrimination properties of the different amide derivatives **7a**–**c** were assayed in ^{1}H NMR experiments towards both racemic ester **9c** and acid **9b** (Figure 2), and the results are presented in Table 1. These substrates were selected because of the presence of the 3,5-dinitrobenzoyl (DNB) group that can not only establish π–π interactions with the electronically complementary aromatic moieties of the isohexide derivatives, which is useful for the enantiodiscrimination, but that also presents some diagnostic signals in a spectral region devoid of proton resonances of the CSAs.

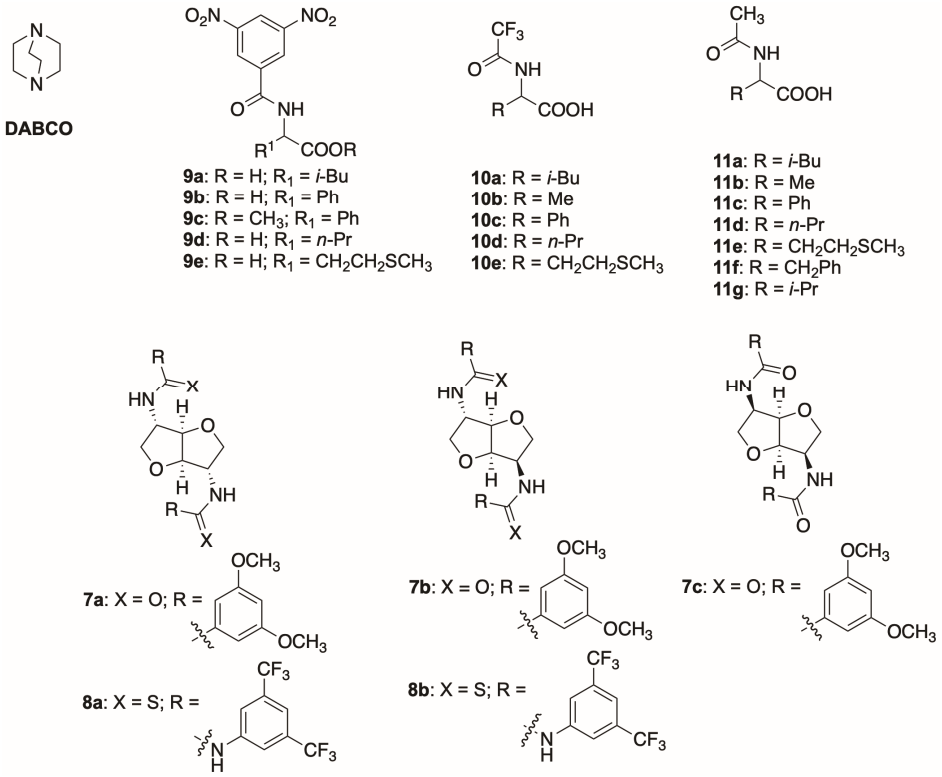

Figure 2. Structures of DABCO, racemic substrates **9a**–**e, 10a**–**e,** and **11a**–**g** and CSAs **7a**–**c** and **8a**–**b**.

Table 1. ^{1}H NMR (500 MHz, $CDCl_3$, 25 °C) nonequivalences (ΔΔδ, ppm) of selected protons of racemic **9b**–**c** (30 mM) in equimolar mixtures with **7a**–**c**.

		ΔΔδ				
CSA	**Substrate**	**NH**	**CH**	***para*-DNB**	***ortho*-DNB**	**CO_2Me**
7a	**9c**	0.013	0.002	0	0.002	0.003
7b	**9c**	0	0.006	0.001	0.002	0
7c	**9c**	0.008	0.005	0	0.002	0
7a	**9b** [1]	0.013	0.007	0.005	0.013	
7b	**9b** [1]	0	0.003	0	0.001	
7c	**9b** [1]	0	0.013	0	0	

[1] In the presence of 1 equivalent of DABCO.

Enantiodiscrimination tests were performed by adding one equivalent of CSA to a 30 mM solution of **9c** in $CDCl_3$ as the solvent. In the case of a substrate having underivatized carboxyl functions, 1,4-diazabicyclo[2,2,2]octane (DABCO) was added as solubilizing agent. The enantiodiscrimination efficiency was evaluated by measuring the chemical shift nonequivalence ($\Delta\Delta\delta = |\Delta\delta_R - \Delta\delta_S| = |(\delta_R - \delta_f) - (\delta_S - \delta_f)| = |\delta_R - \delta_S|$, ppm; where δ_R and δ_S are the chemical shifts of the (*R*)- and (*S*)-enantiomer of the substrate measured in the mixture and δ_f is the chemical shift of the (*R*)- and (*S*)-enantiomer of the free substrate).

All the diamides were able to induce to some extent nonequivalences of selected protons of **9c** and **9b**, which were slightly higher for the NH proton of both substrates in the presence of **7a** and also for the CH in the case of the mixture containing **7c** and **9b** (Table 1). In that way, some influence of the stereochemistry on the enantiodifferentiating properties of these CSAs was demonstrated. On the basis of this first screening, we concluded that amino derivatives of isohexides can be used to prepare CSAs and that diamide **7a**, having the exo–exo stereochemistry of the arylamide moieties, showed the best enantiodiscrimination properties, mainly towards rac-**9b**, having not derivatized carboxylic function. Endo–endo stereochemistry (**7c**) appeared as the least promising.

Enhanced acidity of thiourea function compared to amide one, together with potentiality of 3,5-bis(trifluoromethyl)phenyl moiety as a booster of enantiodiscriminating capabilities, suggested [25–31,33] the possibility of changing the aromatic moiety of the CSA preparing thiourea derivatives **8a**–**b** with exo–exo and exo–endo stereochemistry, respectively. Preliminarily, their efficiency was compared using amino acid derivatives with free carboxylic functionalities, on considering the possibility of introducing suitable probes as *N*-3,5-dinitrobenzoyl (*N*-DNB), N-trifluoroacetyl (*N*-TFA) and *N*-acetyl (*N*-Ac) groups for the detection of enantiodifferentiation as in the cases of **9a**–**b**, **10a**, and 11a, respectively.

The first problem we encountered when using **8a**–**b** as CSAs was the high insolubility of **8a** under the initial conditions, which obliged us not only to work with more dilute samples (5 mM), but also to search for a solvent capable of giving homogeneous samples. After accurately screening (Table S1 in Supplementary Materials) for the best conditions for obtaining complete solubility of the chiral solvating agent, conditions were selected as a 5 mM solution of CSA/rac-**9b**/DABCO (1:1:1) in a 3:7 mixture of CD_2Cl_2/C_6D_6. Although **8b** was highly soluble, the same conditions were used for the sake of comparison. The results reported in Table 2 clearly suggest a higher enantiodiscriminating ability of **8a**–**b** with respect to amide derivatives **7a**–**c**.

Table 2. ^{1}H NMR (600 MHz, 25 °C) nonequivalences ($\Delta\Delta\delta$, ppm) of selected protons of **9a**–**b**, **10a**, and **11a** (5 mM) in equimolar mixtures with **8a**–**b** and DABCO in CD_2Cl_2/C_6D_6 (3:7).

		$\Delta\Delta\delta$				
CSA	**Substrate**	**NH**	***para*-DNB**	***ortho*-DNB**	**CF_3**	**Ac**
8a	**9a**	0	0	0.077		
8b	**9a**	0	0	0.038		
8a	**9b**	0.109	0	0.019		
8b	**9b**	0	0	0.035		
8a	**10a**	0.053			0.010	
8b	**10a**	0			0.020	
8a	**11a**	0.303				0.083
8b	**11a**	0.056				0.040

In spite of the more dilute conditions (5 mM), in comparison with those conditions selected in the case of CSAs **7a**–**c** (30 mM), higher nonequivalences were measured, which was particularly remarkable in the presence of CSA **8a**. Regarding amino acid derivatives, enantiomers of *N*-Ac ones were those that were most efficiently differentiated, with remarkably high nonequivalences of 0.303 ppm and 0.083 ppm for the NH and acetyl groups, respectively (Table 2).

2.1. ^{1}H and ^{19}F Enantiodiscrimination Experiments

To deal with the enantiodiscriminating versatility of **8a** (Figure 2), we extended our analysis to its 5 mM equimolar mixtures with *N*-DNB (**9d**–**e**, Figure 2), *N*-TFA (**10b**–**e**, Figure 2) and *N*-Ac derivatives (**11b**–**g**, Figure 2) in the presence of one equivalent of DABCO. A CD_2Cl_2/C_6D_6 (3:7) solvent mixture was once again selected (see Supplementary Materials).

Very high nonequivalences were detected for the NH and acetyl protons of the *N*-Ac derivatives **11a–g** (Tables 2 and 3), with a maximum value of 0.343 ppm for *N*-acetylphenylglycine derivative **11c**. Lower nonequivalences were obtained for *N*-TFA and *N*-DNB derivatives (Tables 2 and 3).

Table 3. ^{1}H (600 MHz, 25 °C) and ^{19}F (564 MHz, 25 °C) NMR nonequivalences ($\Delta\Delta\delta$, ppm) for **9d–e**, **10b–e**, and **11b–g** (5 mM) in equimolar mixtures with **8a** and DABCO in CD_2Cl_2/C_6D_6 (3:7).

	$\Delta\Delta\delta$				
Substrate	**NH**	***para*-DNB**	***ortho*-DNB**	**CF_3**	**Ac**
9d	0	0	0.029		
9e	0	0.021	0.027		
10b	0.039			0.016	
10c	0.023			0.016	
10d	0.045			0.013	
10e	0			0.010	
11b	0.184				0.066
11c	0.343				0.107
11d	0.189				0.078
11e	0.159				0.069
11f	0.104				0.042
11g	0.257				0.076

Figure 3 shows the relevant spectral regions of the ternary mixtures containing the *N*-acetylamino acids **11b–g**. The spectral regions of the ternary mixtures with **9d–e** and **10b–e** are reported in the Supplementary Materials (Figure S1).

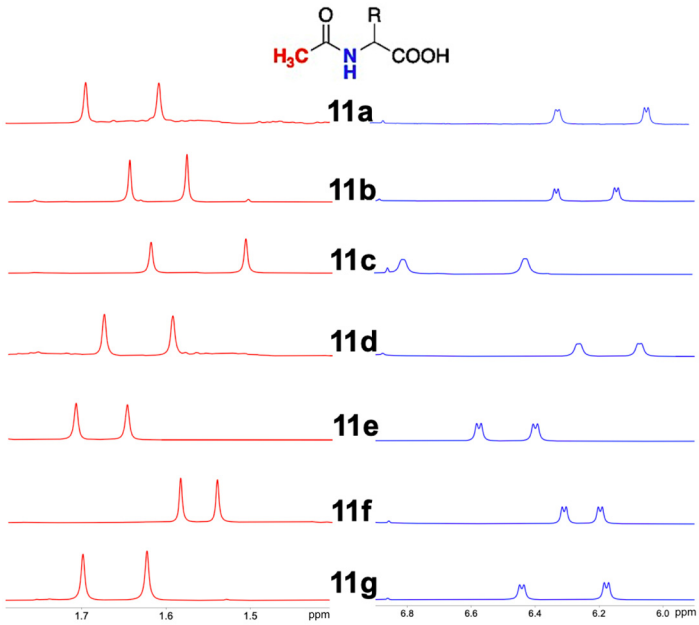

Figure 3. ^{1}H NMR (600 MHz, 25 °C) spectral regions corresponding to the $COCH_3$ (red) and NH (blue) resonances of **11a–g** (5 mM) in equimolar mixtures with **8a** and DABCO in CD_2Cl_2/C_6D_6 (3:7).

Integration of the well separated NH resonances of enantiomeric mixtures of **11a–g** allowed us to accurately determine their relative amounts, leading to values of enantiomeric excesses (ee) in very good agreement with gravimetric data (Figure 4, Table S1 in Supplementary Materials), also in samples with very low (6.4%) and very high (−94.7%) ee, as reported in the case of **11g**.

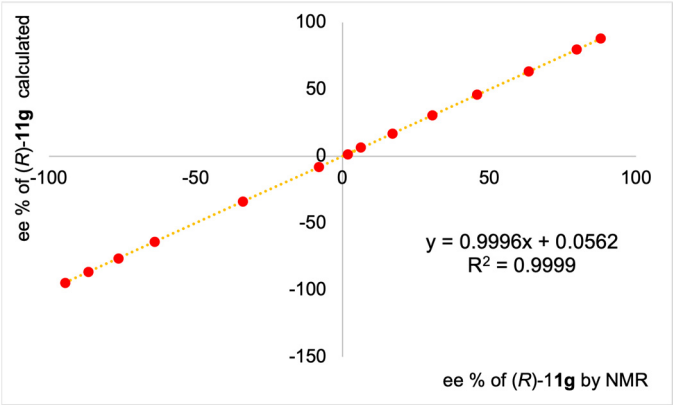

Figure 4. Correlation between the ee% of enantiomerically enriched **11g** (5 mM) in presence of **8a**/DABCO (1:1) in CD_2Cl_2/C_6D_6 (3:7) calculated from gravimetric data and determined by NMR integration of the NH resonance of the substrate.

In the development of new chiral solvating agents based on the selected chiral platform, the guiding idea mainly revolves around expanding enantiodiscriminating capabilities by means of the introduction of functional groups with enhanced potential in terms of establishing a tight network of hydrogen bonds, thereby promoting the thermodynamic stabilization of diastereomeric solvates. Therefore, it was imperative to compare the capabilities of the most efficient thiourea-based CSA, i.e., **8a**, with those of the corresponding urea system **12a**. Consequently, we synthesized urea **12a** by reacting diamine **6a** with 3,5-bis(trifluoromethyl)phenyl isocyanate and we assessed its ability to differentiate the proton nuclei of selected enantiomeric substrates, particularly **9a**, **9b**, **10a**, and **11a** (Table 4) For the chiral urea, auxiliary exacerbating solubility issues were found compared to the thiourea counterpart, making it challenging to achieve complete solubilization at a concentration of 5 mM. Therefore, comparative measurements between the two systems were conducted at a concentration of 2 mM, at which **12a** proved to be completely solubilized in the mixtures. In all instances, the urea-based CSA produced significantly lower nonequivalence data compared to the thiourea CSA (Table 4).

Table 4. ^{1}H NMR (600 MHz, 25 °C) nonequivalences ($\Delta\Delta\delta$, ppm) of selected protons of racemic **9a-b**, **10a**, and **11a** (2 mM) in equimolar mixtures with **8a** or **12a** and DABCO in CD_2Cl_2/C_6D_6 3:7.

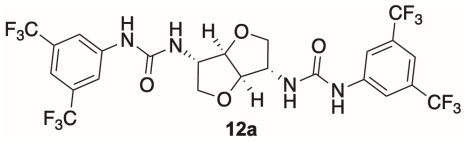

			$\Delta\Delta\delta$			
CSA	**Substrate**	**NH**	***para*-DNB**	***ortho*-DNB**	**Ac**	**CF_3**
8a	**9a**	0.107	0.003	0.044		
12a	**9a**	0.040	0	0.018		
8a	**9b**	0.086	0.008	0.021		0
12a	**9b**	0.016	0	0		
8a	**10a**	0.055				0.009
12a	**10a**	0				0
8a	**11a**	0.419			0.079	
12a	**11a**	0.163			0.016	

2.2. ^{1}H NMR Configurational Assignment

Only a few CSAs have been so far reported for configurational assignments [31,41–43], as CDAs have been preferred in this field since the earliest reports of Mosher in 1963 [44]. As

a matter of fact, CDAs may produce higher nonequivalences and originate more conformationally restricted diastereomeric derivatives compared to CSAs. This last feature favors the building of molecular models suited for the rationalization of the correlation between the relative positions of diastereomeric derivatives signals and their absolute configuration. The fixed skeleton of **8a** suggested that it would be worthwhile to explore its use for the configurational assignment of acetyl derivatives of amino acids, in consideration of the remarkable enantiodifferentiation detected in the mixtures **8a**/*N*-Ac-derivative/DABCO. Availability of only one stereoisomer of the CSA required the analysis of enantiomerically enriched samples in order to evaluate the sense of nonequivalence, i.e., the relative positions of enantiomeric signals in enantiomerically enriched samples having known absolute configurations.

As shown in Table S2 in Supplementary Materials, for every derivative **11a–c**,**f**,**g**, the proton resonances of the NH and Ac groups of the (*R*)-enantiomer were shifted at a higher frequency with respect to those due to the (*S*)-enantiomer in the presence of the CSA (Figure 5).

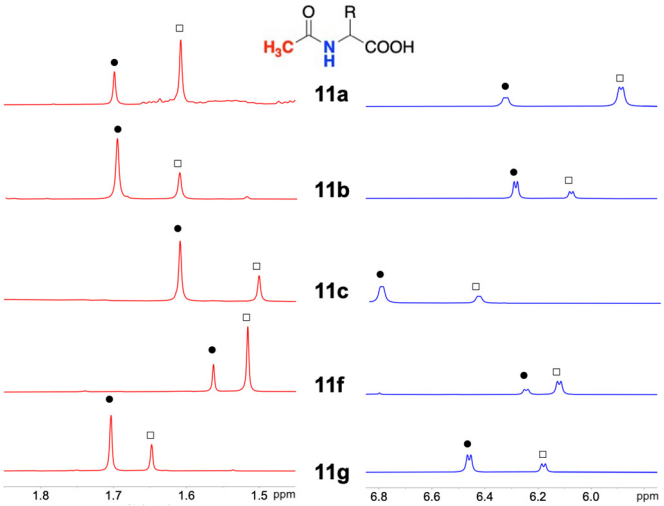

Figure 5. ^{1}H NMR (600 MHz, 25 °C) spectral regions corresponding to the $COCH_3$ (red) and NH (blue) resonances of enantiomerically enriched **11a–c**,**f**,**g** in the presence of **8a**/DABCO (1:1) in CD_2Cl_2/C_6D_6 (3:7). • and □ indicate (*R*)- and (*S*)-acetylamino acid resonances, respectively.

Therefore, a reproducible correlation between the sense of nonequivalence and the absolute configuration has been obtained, and this correlation can be reliably extended to samples having an unknown absolute configuration, provided that at least a minimum amount of the defect enantiomer is present in the mixture.

2.3. Investigation of Chiral Recognition Processes

The chemical bases of the chiral recognition process were investigated in the mixtures containing **8a** and one of each enantiomer of **11g** in the presence of DABCO by 1D or 2D ROESY in order to detect intra- and intermolecular dipolar interactions (Figures S3–S7, S9, and S10 in Supplementary Materials).

The complexation stoichiometries were preliminarily defined using Job's method in samples having different substrate to CSA ratios while keeping constant the total concentration (Tables S2 and S3 in Supplementary Materials). Graphs reporting the normalized complexation shift of the acetyl protons of the substrate as a function of the molar fraction of **8a** showed a symmetrical bell curve with a well-defined maximum at a 0.5 molar fraction for the diastereomeric complex containing (*S*)-**11g**, according to a 1-to-1 complexation stoichiometry (Figure S2 in Supplementary Materials). Otherwise, a well-defined maximum at the 0.3 molar fraction was obtained in the case of (*R*)-**11g**, demonstrating a 1-to-2 CSA/substrate complexation stoichiometry (Figure S2 in Supplementary Materials).

Very low solubility of the CSA did not allow us to obtain reliable values of the association constants of the two diastereomeric complexes.

Investigation of the stereochemical features of the diastereomeric complexes started from the definition of the conformations of **8a** and **11g** in both ternary mixtures.

Identical intramolecular ROE interactions were detected for **8a** in the two mixtures (Figure S4, Supplementary Materials), indicating that **8a**'s conformation was the same in both solvates. In particular, regarding protons NH-7 and NH-11 (Figure S4 in Supplementary Materials), the intensity of ROE effects at the frequencies of methine protons H_1 and H_4 were higher than ROE effects at methylene protons H_{3a}/H_{6a}. Lower dipolar interactions were detected at H_2 and H_5. On this basis, a transoid arrangement of the thiourea protons NH-7/NH-11 and H_2/H_5 can be assessed. Intense intra-ROE effects between the amide protons (Figure S5 in Supplementary Materials) supported a cisoid arrangement of these protons in the thiourea fragment (Figure 6) that was further corroborated by the absence of ROE effect between NH-7/NH-11 and protons of 3,5-bis(trifluoromethyl)phenyl groups (Figure S4 in Supplementary Materials).

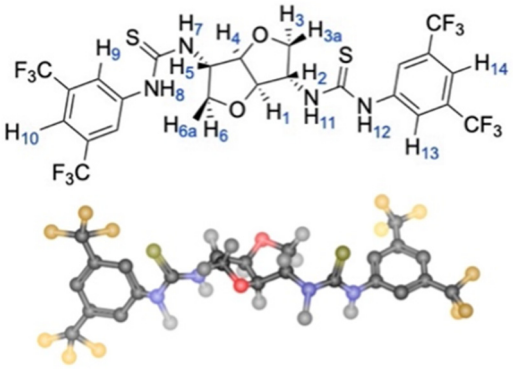

Figure 6. Conformation of **8a** in the ternary mixtures (*R*)- and (*S*)-**11g**/**8a**/DABCO in CD_2Cl_2/C_6D_6 (3:7) according to NMR data.

The conformation of **11g** was also the same in the two mixtures. A transoid arrangement of methine proton H_A and amide proton NH-B was suggested by very low-intensity H_A/NH-B ROE effect compared to the very high-intensity of H_A/H_D ROE (Figures S6 and S7 in Supplementary Materials). The dihedral angle defined by the fragment H_A-C-N-H_B was accordingto data, as a J_{HAHB} of 8.0 Hz and 8.5 Hz was measured for (*R*)- and (*S*)-**11g**, respectively, corresponding [45] to very similar values of the dihedral angles of 147.1° and 150.5° for (*R*)- and (*S*)-**11g**, respectively. The conformation of **11g** in mixture is shown in Figure S8 in Supplementary Materials.

The analysis of intermolecular ROE effects allowed us to impose proximity constraints that were significantly differentiated in the two mixtures.

In particular, very different intermolecular dipolar interactions were originated by H_1 and H_4 of **8a**, which were the sole protons of the CSA producing ROE effects with the protons of enantiomeric substrates (Figure S9 in Supplementary Materials). Therefore, both (*R*)-**11g** and (*S*)-**11g** interacted with the convex surface of the CSA, including protons H_1 and H_4 of the bicycle and the NH protons of the thiourea moieties. However, H_1 and H_4 showed a more intense ROE at the H_A proton of (*S*)-**11g** and a less intense effect at its acetyl group (Figure S9 in Supplementary Materials). The reverse was found for the mixture containing (*R*)-**11g**, with the major ROE effect observed at the acetyl protons (Figure S9 in Supplementary Materials).

Therefore, the (*S*)-enantiomer interacted with the chiral auxiliary, placing the carbonyl functions (acetyl and carboxylate) close to NH-7 and NH-11 groups in a spatial arrangement allowing to place the most sterically demanding group (isopropyl), away from the interaction site, as shown in Figure 7. Accordingly, the acetyl group of (*S*)-**11g** was in

spatial proximity to *ortho*-protons of the phenyl moiety of **8a** (Figure S10 in Supplementary Materials). This interaction model was according to the 1-to-1 complexation stoichiometry.

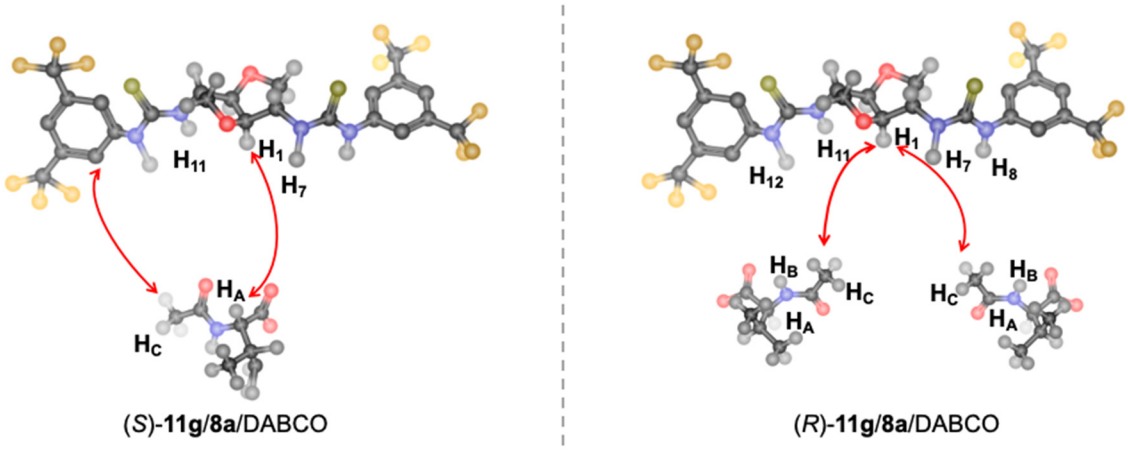

Figure 7. 3D schematic representation of diastereomeric complexes (*S*)-**11g**/**8a**/DABCO and (*R*)-**11g**/**8a**/DABCO. The arrows indicate the more relevant ROE effects detected in the corresponding diastereomeric complexes.

Due to the 1-to-2 CSA to substrate complexation stoichiometry in the mixture containing (*R*)-**11g** and the spatial proximity of the methyl group of the acetyl of (*R*)-**11g** and H_1 and H_4 protons of **8a** (Figure S10 in Supplementary Materials), placing its carbonyl functional group far away from the CSA surface, a different interaction model can be hypothesized in which the main stabilizing interaction must necessarily involve the carboxylate group of two amino acid units with each one interacting with one bis-thiourea moiety as depicted in Figure 7.

Interestingly, DABCO protons produced intense ROE contacts with protons of the CSA and protons of each amino acid derivative enantiomer (Figure S4 in Supplementary Materials), supporting its role in the stabilization of the two diastereomeric solvates, which goes beyond its solubilizing effect. DABCO acts as a bridge between the polar groups of the two components.

The mediating role of DABCO became evident through a comparison of its diffusion coefficient (D, m^2s^{-1}) measured by diffusion-ordered spectroscopy experiments in the pure state and its binary mixture containing the chiral auxiliary, along with ternary systems that also included the two enantiomers of the acetyl derivative of valine **11g**. Starting from the initially high value of pure DABCO (D = 21.2×10^{-10} m^2s^{-1}), as expected for its small molecular size, the chiral auxiliary itself initiated attractive interactions, resulting in a reduction of the diffusion coefficient of DABCO by 5 units (D = 16.3×10^{-10} m^2s^{-1}). An even more pronounced decrease in the diffusion coefficient of DABCO was observed in mixtures (*R*)-**11g**/CSA/DABCO and (*S*)-**11g**/CSA/DABCO, reaching values of 6.7×10^{-10} m^2s^{-1} and 7.4×10^{-10} m^2s^{-1}, respectively, which highlights the cooperative function of DABCO in the formation of the two diastereomeric solvates.

Therefore, according to interaction models described above, strongly differentiated chemical environments are felt by the acetyl and amide protons of the two enantiomers leading to their highly differentiated chemical shifts.

3. Materials and Methods

3.1. Materials

All syntheses of sensitive compounds were realized under dry Argon in flame-dried lab glassware. Reactants and reagents, if not specified, were commercially available and used as received For the synthesis of sensitive compounds, dry CH_2Cl_2 and THF obtained using a MB-SPS solvent purification system were used. Pyridine was distilled under inert

atmosphere over CaH_2, and 3,5-bis(trifluoromethyl)phenyl isothiocyanate was distilled under vacuum.

3.2. Methods

Analytical thin layer chromatography (TLC) was performed on ALUGRAM Xtra G/UV254 plates (Macherey-Nagel GmbH & Co.KG, Duren, Germany) and detection of compounds was performed with a UV lamp and permanganate or sulfuric vanillin solution. Melting points were measured on a Buchi Melting Point B-545 instrument (BUCHI Italia s.r.l, Cornaredo, Italy), optical rotations were measured on a 1 dm cell at the sodium D line on an Anton Paar MCP 300 Polarimeter or on an Jasco Polarimeter. NMR characterization of the bis-amides **7a**–**c** and corresponding intermediates and the enantiodiscrimination experiments with **7a**–**c** were carried out on a spectrometer operating at 500 or 400 MHz, 126, or 101 MHz for ^{1}H and ^{13}C nuclei, respectively; the NMR characterization of bis-thioureas **8a**–**b** and *N*-acetylamino acids and the enantiodiscrimination experiments with **8a**–**b** were carried out using a spectrometer operating at 600 MHz, 150 MHz, and 564 MHz for ^{1}H, ^{13}C, and ^{19}F nuclei, respectively. The samples were analyzed in a $CDCl_3$, DMSO-d_6, or methanol-d_4 solution. ^{1}H and ^{13}C chemical shifts were referenced to tetramethyl silane (TMS) as the secondary reference standard; ^{19}F chemical shifts were referenceed against $CFCl_3$ and trifluoro-toluene (**8a**–**8b**) as the external standard with temperature control (25 $\pm$ 0.1 and 21 $\pm$ 0.1 °C for the spectrometer operating at 600 and 400 or 500 MHz, respectively). A 1 s relaxation delay and 200 increments of 4 transients, each with 2*K*-points, were employed for gCOSY (gradient Correlation SpectroscopY) and TOCSY (Total COrrelation SpectroscopY) experiments. The mixing time for TOCSY maps was 80 ms. The 2D-ROESY (Rotating-frame Overhauser Enhancement SpectroscopY) experiments were carried out with a relaxion time of 1 s, a mixing time of 0.3 s, and 128 increments of 8 transients, with 2*K*-points. For 1D-ROESY spectra, a selective inversion pulse was employed with transients ranging from 512 to 1024, a relaxion delay of 1 s, and a mixing time of 0.5 s. The gHSQC (gradient Heteronuclear Single Quantum Coherence) and the gHMBC (gradient Heteronuclear Multiple Bond Correlation) spectra were recorded with a relaxion time of 1.2 s and 128–200 increments with 16–32 transients, each with 2*K*-points. The gHMBC experiments were optimized for a long-range coupling constant of 8 Hz. For DOSY (Diffusion-Ordered Spectroscopy) experiments, a stimulated echo sequence with self-compensating gradient schemes and 64 K data points was used. Typically, g was varied in 20 steps (2–32 transients each), and Δ and δ were optimized to obtain an approximately 90–95% decrease in resonance intensity at the largest gradient amplitude. Baselines of arrayed spectra were corrected prior to processing the data. After data acquisition, each FID was apodized with 1.0 Hz line broadening and then Fourier transformed. DOSY macro was used for data processing. The assignments of ^{1}H NMR and ^{13}C NMR chemical shifts for **8a**–**b**, reported below, are shown in Figures SI32, SI33, SI34, and SI35 in Supplementary Materials; the NMR data were described using the following abbreviations: s—singlet, d—doublet, dt—double doublet, ddd—double double douplet, t—triplet, q—quartet, and m—multiplet.

3.3. General Procedures for the Synthesis of the bis-Amides **7a**–**c**

To a solution of diamine (1.0 mmol) in dry pyridine (5 mL), 3,5-dimethoxybenzoyl chloride (421 mg, 2.1 mmol) was added. The suspension was stirred for 6 h at room temperature and the reaction was monitored by TLC analysis (CH_2Cl_2/Acetone/HCOOH 85:15:1). Then, water (10 mL) was added and the mixture was extracted with CH_2Cl_2 (3 $\times$ 10 mL). The organic phases were combined and washed sequentially with 10% aqueous HCl (10 mL), H_2O (10 mL), saturated $NaHCO_3$ (10 mL), and again with H_2O (10 mL). The organic phase was dried over anhydrous Na_2SO_4. The solvent was removed under reduced pressure to give the crude product.

3.3.1. *N,N′*-((3*S*,3a*R*,6*S*,6a*R*)-Hexahydrofuro[3,2-b]furan-3,6-diyl)bis(3,5-dimethoxybenzamide), (**7a**)

The product was purified by flash chromatography (silica gel, CH_2Cl_2/Acetone/HCOOH 85:15:1) to give 189 mg (0.4 mmol, 39%) of a pure white solid. Mp = 75–77 °C. $[\alpha]_D^{20}$ = +50.2 (c = 0.55; Acetone); ^{1}H NMR (500 MHz, $CDCl_3$, 21 °C, TMS, ppm) δ: 6.84 (d, *J* = 2.3 Hz, 4H), 6.57 (t, *J* = 2.3 Hz, 2H), 6.17 (d, *J* = 7.3 Hz, 2H), 4.71 (s, 2H), 4.62 (ddd, *J* = 6.9 Hz, *J* = 4.6 Hz, *J* = 2.0 Hz, 2H), 4.10–4.04 (m, 2H), 3.92 (dd, *J* = 9.9 Hz, *J* = 2.0 Hz, 2H), 3.80 (s, 12H). ^{13}C{^{1}H} NMR (101 MHz, $CDCl_3$, 21 °C, TMS, ppm) δ: 167.1, 161.1, 136.0, 105.0, 104.0, 86.4, 72.5, 57.1, and 55.7.

3.3.2. *N,N′*-((3*R*,3a*R*,6*S*,6a*R*)-Hexahydrofuro[3,2-b]furan-3,6-diyl)bis(3,5-dimethoxybenzamide), (**7b**)

The product was purified by flash chromatography (silica gel, CH_2Cl_2/Acetone/HCOOH 85:15:1) to give 142 mg (0.3 mmol, 32%) of a white solid. Mp = 192–193 °C. $[\alpha]_D^{25}$ = +51.2 (c = 0.46; $CHCl_3$). ^{1}H NMR (500 MHz, $CDCl_3$, 21 °C, TMS, ppm) δ: 6.90 (d, *J* = 2.2 Hz, 2H), 6.85 (d, *J* = 2.2 Hz, 2H), 6.64 (d, *J* = 7.2 Hz, 1H), 6.58 (q, *J* = 2.5 Hz, 2H),), 6.19 (d, *J* = 7.3 Hz, 1H), 4.67 (m, 4H), 4.30 (dd, *J* = 8.8 Hz, *J* = 7.2 Hz, 1H), 4.10 (dd, *J* = 9.8 Hz, *J* = 4.7 Hz, 1H), 4.00–3.94 (m, 1H), 3.82 (s, 12H), 3.51 (dd, *J* = 16.0 Hz, *J* = 8.5 Hz, 1H). ^{13}C{^{1}H} NMR (126 MHz, $CDCl_3$, 21 °C, TMS, ppm) δ 167.4, 167.1, 161.1, 161.0, 136.1, 136.0, 105.1, 105.0, 103.9, 103.7, 87.0, 81.6, 73.5, 71.7, 57.9, 55.7, and 53.3.

3.3.3. *N,N′*-((3*R*,3a*R*,6*R*,6a*R*)-Hexahydrofuro[3,2-b]furan-3,6-diyl)bis(3,5-dimethoxybenzamide), (**7c**)

The product was purified by flash chromatography (silica gel, CH_2Cl_2/Acetone 9:1) to give 142 mg (0.3 mmol, 30%) of a white foamy solid. Mp = 168 °C. $[\alpha]_D^{25}$ = +119.4 (c = 0.69; $CHCl_3$). ^{1}H NMR (400 MHz, $CDCl_3$, 21 °C, TMS, ppm) δ: 6.90 (d, *J* = 2.3 Hz, 4H), 6.71 (d, *J* = 7.1 Hz, 2H), 6.58 (t, *J* = 2.3 Hz, 2H), 4.78–4.67 (m, 4H), 4.40 (t, *J* = 7.9 Hz, 2H), 3.82 (s, 12H), 3.52–3.46 (m, 2H). ^{13}C{^{1}H} NMR (126 MHz, $CDCl_3$, 21 °C, TMS, ppm) δ: 167.4, 161.0, 131.9, 105.2, 103.8, 82.0, 72.6, 55.7, and 54.0.

3.4. General Procedures for the Synthesis of the bis-Thioureas **8a**–**b**

To a solution of diamine (154.0 mg, 1.1 mmol) in dry THF (10 mL), 3,5-bis (trifluoromethyl)phenyl isothiocyanate 370 μL (1.9 mmol) was added. The mixture was stirred overnight at room temperature and the reaction was monitored by TLC analysis ($CHCl_3$/MeOH 9:1). The solvent was removed under reduced pressure to obtain the crude product.

3.4.1. 1,1′-((3*S*,3a*R*,6*S*,6a*R*)-Hexahydrofuro[3,2-b]furan-3,6-diyl)bis(3-(3,5-bis(trifluoromethyl)phenyl)thiourea), (**8a**)

The solid was recrystallized by Acetone-Hexane obtaining 511 mg (0.8 mmol, 70%) of a white powder. Mp = 173–175 °C. $[\alpha]_D^{20}$ = −22.9 (c = 0.35; MeOH). ^{1}H NMR (600 MHz, [D_6]DMSO, TMS, 25 °C, ppm) δ: 9.94 (s, 2H), 8.57 (s, 2H), 8.22 (s, 4H), 7.76 (s, 2H), 4.69 (s, 2H), 4.64 (s, 2H), 4.00 (dd, *J* = 9.8 Hz, *J* = 4.8 Hz, 2H), 3.84 (d, *J* = 9.8 Hz, 2H). ^{13}C{^{1}H} NMR (150 MHz, [D_6]DMSO, TMS, 25 °C, ppm) δ: 180.6 (*C*=S), 141.6 (*C*-Ar), 130.0 (q, *J* =33.0 Hz, *C*-CF_3), 123.7 (q, *J* = 272.9 Hz, CF_3), 122.2 (*C*-Ar), 116.3 (*C*-Ar), 85.5 (CH), 71.3 (CH_2), 60.3 (CH). ^{19}F NMR (564 MHz, [D_6]DMSO, trifluoro-toluene, ppm) δ: −0.47.

3.4.2. 1,1′-((3*R*,3a*S*,6*S*,6a*R*)-Hexahydrofuro[3,2-b]furan-3,6-diyl)bis(3-(3,5-bis(trifluoromethyl)phenyl)thiourea), (**8b**)

The product was purified by chromatography (silica gel, $CHCl_3$/Acetone 8:2) to give 479.1 mg (0.7 mmol, 66%) of a yellow powder. Mp = 92–97 °C. $[\alpha]_D^{20}$ = + 297 (c = 0.01; EtOH). ^{1}H NMR (600 MHz, [D6]DMSO, TMS, 25 °C, ppm) δ: 10.45 (s, 1H), 9.98 (s, 1H), 8.57 (s, 1H), 8.29 (s, 2H), 8.22 (s, 2H), 8.11 (d, *J* = 7.2 Hz, 1H), 7.74 (s), 4.80 (q, *J* = 7.3 Hz, 1H), 4.73 (m, 2H), 4.64 (d, *J* = 4.0 Hz, 1H), 4.13 (t, *J* = 8.0 Hz, 1H), 4.03 (dd, *J* = 9.7 Hz, *J* = 4.7 Hz, 1H), 3.92

(m, 1H), 3.47 (t, *J* = 8.7 Hz, 1H). $^{13}C\{^1H\}$ NMR (150 MHz, [D_6]DMSO, TMS, 25 °C, ppm) δ: 181.2 (*C*=S), 181.0 (*C*=S), 142.2 (*C*-Ar), 130.1 (m, *C*-CF_3), 123.7 (q, J = 271.4 Hz, CF_3), 122.7 (*C*-Ar), 122.1 (*C*-Ar), 116.8 (*C*-Ar), 86.7 (CH), 81.2 (CH), 73.1 (CH_2), 70.3 (CH_2), 61.7 (CH), 57.5 (CH). ^{19}F NMR (564 MHz, [D_6]DMSO, trifluoro-toluene, ppm) δ: −0.46 and −0.49.

*3.5. 1,1′-((3S,3aR,6S,6aR)-Hexahydrofuro[3,2-b]furan-3,6-diyl)bis(3-(3,5-bis(trifluoromethyl)phenyl)urea), (**12a**)*

To a solution of diamine (280 mg, 1.94 mmol) in dry THF (18 mL), 3,5-bis (trifluoromethyl)phenyl isocyanate (740 µL, 2.2 mmol) was added. The mixture was stirred overnight at room temperature and the reaction was monitored by TLC analysis ($CHCl_3$/MeOH 9:1). The solvent was removed under reduced pressure to obtain the product (1.74 mmol, 90%). ^1H NMR (600 MHz, [D_6]DMSO, TMS, 25 °C, ppm) δ: 9.07 (s, 2H), 8.16 (s, 4H), 7.54 (s, 2H), 6.89 (d, *J* = 6.8 Hz, 2H), 4.50 (s, 2H), 4.08 (m, 2H), 3.89 (dd, *J* = 9.5 Hz, *J* = 5.1 Hz, 2H), 3.69 (dd, *J* = 9.5 Hz, *J* = 1.8 Hz, 2H). $^{13}C\{^1H\}$ NMR (150 MHz, [D_6]DMSO, TMS, 25 °C, ppm) δ: 154.9 (*C*=O), 141.6 (*C*-Ar), 131.2 (q, *J* =32.8 Hz, *C*-CF_3), 123.8 (q, *J* = 273.0 Hz, CF_3), 118.1 (*C*-Ar), 114.3 (*C*-Ar), 86.6 (CH), 71.2 (CH_2), 56.8 (CH).

4. Conclusions

New U-, N-, and W-shaped arylamides and arylthioureas CSAs **7a**–**c** and **8a**–**b** were easily synthesized starting with commercially available isomannide and isosorbide. The stereospecific interconversion of the hydroxyls of the two natural isohexides allowed us to obtain the three amino derivatives having isomannide, isosorbide, and isoidide stereochemistry, which were easily transformed into the corresponding arylamides, and arylthioureas. In view of the biological relevance of amino acids, their *N*-DNB, *N*-TFA, and *N*-Ac derivatives were probed as chiral substrates in the enantiodiscrimination experiments, highlighting the finding that bis-thiourea CSA **8a** with 3,5-bis(trifluoromethyl)phenyl moieties in an exo–exo stereochemistry was endowed with remarkable enantiodiscriminating power towards *N*-acetylamino acids, surpassing that of the corresponding urea derivative **12a**. The nature of the probe signals (doublets for NH and singlets for Ac) of the chiral substrates allowed us to also attain accurate determinations of enantiomeric compositions in diluted mixtures with very high or very low enantiomeric excesses. Importantly, **8a** constitutes one of the few cases of the use of CSAs for configurational assessments. It is likely that the flexible lateral arms of the CSA in an open conformation can act in synergy to grab a single substrate unit. Alternatively, they can act independently while grabbing two of them in response to steric-repulsive effects. In that way, an efficient enantiomeric differentiation can be attained. As a matter of fact, alternative exo–endo stereochemistry, in which thiourea moieties cannot cooperate in the interaction with the chiral substrates, produces lower enantiomer differentiations in the NMR spectra. Therefore, anisohexide skeleton constitutes a versatile chiral platform for the design of new chiral auxiliaries bearing different kinds of functional groups to be applied to the enantiodiscrimination of different classes of chiral substrates.

Supplementary Materials: The following supporting information can be downloaded at https://www.mdpi.com/article/10.3390/molecules29061307/s1. Figure SI1, ^1H NMR spectrum of diphenyl (3*S*,3a*R*,6*S*,6a*R*)-hexahydrofuro[3,2-b]furan-3,6-dicarboxylate; Figure SI2, $^{13}C\{^1H\}$ spectrum of diphenyl (3*S*,3a*R*,6*S*,6a*R*)-hexahydrofuro[3,2-b]furan-3,6-dicarboxylate; Figure SI3, ^1H NMR spectrum of **3**; Figure SI4, $^{13}C\{^1H\}$ NMR spectrum of **3**; Figure SI5, ^1H NMR spectrum of **4a**; Figure SI6, $^{13}C\{^1H\}$ NMR spectrum of **4a**; Figure SI7, ^{19}F NMR spectrum of **4a**; Figure SI8, ^1H NMR spectrum of **4b**; Figure SI9, $^{13}C\{^1H\}$ NMR spectrum of **4b**; Figure SI10, ^{19}F NMR spectrum of **4b**; Figure SI11, ^1H NMR spectrum of **4c**; Figure SI12, $^{13}C\{^1H\}$ NMR spectrum of **4c**; Figure SI13, ^{19}F NMR spectrum of **4c**; Figure SI14, ^1H NMR spectrum of **5a**; Figure SI15, $^{13}C\{^1H\}$ NMR spectrum of **5a**; Figure SI16, ^1H NMR spectrum of **5b**; Figure SI17, $^{13}C\{^1H\}$ NMR spectrum of **5b**; Figure SI18, ^1H NMR spectrum of **5c**; Figure SI19 $^{13}C\{^1H\}$ NMR spectrum of **5c**; Figure SI20, ^1H NMR spectrum of **6a**; Figure SI21, $^{13}C\{^1H\}$ NMR spectrum of **6a**; Figure SI22, ^1H NMR spectrum of **6b**; Figure SI23, $^{13}C\{^1H\}$ NMR spectrum of **6b**; Figure SI24, ^1H NMR spectrum of **6c**; Figure SI25, $^{13}C\{^1H\}$ NMR spectrum of **6c**;

Figure SI26, ^{1}H NMR spectrum of **7a**, Figure SI27, ^{13}C{^{1}H} NMR spectrum of 7a; Figure SI28, ^{1}H NMR spectrum of **7b**; Figure SI29, ^{13}C{^{1}H} NMR spectrum of **7b**; Figure SI30, ^{1}H NMR spectrum of **7c**; Figure SI31, ^{13}C{^{1}H} NMR spectrum of **7c**; Figure SI32, ^{1}H NMR spectrum of **8a**; Figure SI33, ^{13}C{^{1}H} NMR spectrum of **8a**, Figure SI34, ^{1}H NMR spectrum of **8b**; Figure SI35, ^{13}C{^{1}H} NMR spectrum of **8b**; Table SI1, Nonequivalence for racemic **11a** in equimolar mixtures **11a**/**8a**/DABCO in different solvents; Figure S1, Nonequivalences of **9c**–**d** and **10b**–**e** in equimolar mixtures with **8a** and DABCO; Figure S2, Complexation stoichiometry of (R)-11g/8a/DABCO (left) and (S)-11g/8a/DABCO (right) based on the 1H resonances of the acetyl group of 11g; Table S1, Enantiomeric purity determination; Table S2, Complexation shift of **11a**–**c**,**11f**, **11g** in equimolar mixtures with **8a** and DABCO; Table S3, Chemical shift of Ac protons of (*S*)-**11g** in the mixture (*S*)-**11g/8a**/DABCO; Table S4, Chemical shift of Ac protons of (*R*)-**11g** in the mixture (*R*)-**11g/8a**/DABCO; Figure S3, ^{1}H NMR spectra of the equimolar (5 mM) mixtures (*R*)-**11g**/**8a**/DABCO (*S*)-**11g**/ **8a**/DABCO; Figure S4, 2D ROESY maps of the equimolar (5 mM) mixtures (*R*)-**11g**/**8a**/DABCO (*S*)-**11g**/ **8a**/DABCO; Figure S5, 1D ROESY spectra of NH-8/NH-12 of (*R*)-**11g** (5 mM) in the equimolar (*R*)-**11g**/DABCO/**8a**; Figure S6, 1D ROESY spectra of H_A of (*R*)-**11g** (5 mM) in the mixture (*R*)-**11g**/DABCO/**8a**; Figure S7, 1D ROESY spectra of the proton H_B of (*R*)-**11g** (5 mM) in the mixture (*R*)-**11g**/DABCO/**8a**; Figure S8, 3D representation of (*R*)-**11g**; Figure S9, 1D ROESY spectra of H_1 and H_4 of (*R*)-/(*S*)-**11g** (5 mM) in the mixture (*R*)-/(*S*)-**11g**/DABCO/**8a**; Figure S10, 1D ROESY spectra of H_c of (*R*)-/(*S*)-**11g** (5 mM) in the mixture (*R*)-/(*S*)-**11g**/DABCO/**8a**. Refs [46–51] are cited in Supplementary Materials.

Author Contributions: Conceptualization, A.I., F.B., and G.U.B.; methodology, F.B. and G.U.B.; validation, F.C. and C.B.; formal analysis, F.C. and C.B.; investigation, F.C., V.Z. and C.B.; data curation, F.C. and C.B.; writing—original draft preparation, F.C., A.I., F.B., C.B. and G.U.B.; writing—review and editing, F.C., A.I., F.B., C.B., V.Z. and G.U.B.; visualization, F.C. and C.B.; supervision, A.I., F.B. and G.U.B.; project administration, A.I. and G.U.B.; funding acquisition, A.I. and G.U.B. All authors have read and agreed to the published version of the manuscript.

Funding: This research was supported by the Università di Pisa under the "PRA–Progetti di Ricerca di Ateneo" (Institutional Research Grants), Project no. PRA_2022–2023_ "New challenges of transition metal and lanthanide complexes in the perspective of green chemistry".

Institutional Review Board Statement: Not applicable.

Informed Consent Statement: Not applicable.

Data Availability Statement: Data are contained within the article and Supplementary Materials.

Conflicts of Interest: The authors declare no conflicts of interest.

References

1. De Luca, C.; Felletti, S.; Franchina, F.A.; Bozza, D.; Compagnin, G.; Nosengo, C.; Pasti, L.; Cavazzini, A.; Catani, M. Recent developments in the high-throughput separation of biologically active chiral compounds via high performance liquid chromatography. *J. Pharm. Biomed. Anal.* **2024**, *238*, 115794. [CrossRef] [PubMed]
2. Qian, H.-L.; Xu, S.-T.; Yan, X.-P. Recent advances in separation and analysis of chiral compounds. *Anal. Chem.* **2023**, *95*, 304–318. [CrossRef] [PubMed]
3. Peluso, P.; Chankvetadze, B. Recognition in the domain of molecular chirality: From noncovalent interactions to separation of enantiomers. *Chem. Rev.* **2022**, *122*, 13235–13400. [CrossRef]
4. Cagliero, C.; Sgorbini, B.; Cordero, C.; Liberto, E.; Runiolo, P.; Bicchi, C. *Separation Science: Gas Chromatography*, 2nd ed.; Elsevier: Amsterdam, The Netherlands, 2021; Chapter 23. [CrossRef]
5. Casado, N.; Valimana-Traverso, J.; Garcia, M.A.; Marina, M.L. Enantiomeric determination of drugs in pharmaceutical formulations and biological samples by electrokinetic chromatography. *Crit. Rev. Anal. Chem.* **2020**, *50*, 554–584. [CrossRef]
6. Leung, D.; Kang, S.O.; Anslyn, E.V. Rapid determination of enantiomeric excess: A focus on optical approaches. *Chem. Soc. Rev.* **2012**, *41*, 448–479. [CrossRef]
7. Zhou, X.; Wang, Z.; Li, S.; Rong, X.; Bu, J.; Liu, Q.; Ouyang, Z. Differentiating enantiomers by directional rotation of ions in a mass spectrometer. *Science* **2024**, *383*, 612–618. [CrossRef] [PubMed]
8. Hu, M.; Yuan, Y.-X.; Wang, W.; Li, D.-M.; Zhang, H.-C.; Wu, B.-X.; Liu, M.; Zheng, Y.-S. Chiral recognition and enantiomer excess determination based on emission wavelength change of AIEgen rotor. *Nat. Commun.* **2020**, *11*, 2274. [CrossRef]
9. Pu, L. Enantioselective fluorescent recognition of free amino acids: Challenges and opportunities. *Angew. Chem. Int. Ed.* **2020**, *59*, 21814–21828. [CrossRef]
10. Domingos, S.R.; Pérez, C.; Marshall, M.D.; Leung, H.O.; Schnell, M. Assessing the performance of rotational spectroscopy in chiral analysis. *Chem. Sci.* **2020**, *40*, 10863–10870. [CrossRef]

11. Balzano, F.; Uccello-Barretta, G.; Aiello, F. Chiral Analysis: Advances in Spectroscopy, Chromatography and Emerging Methods. In *Chiral Analysis*, 2nd ed.; Polavarapu, P.L., Ed.; Elsevier: Amsterdam, The Netherlands, 2018; Chapter 9; pp. 367–427. [CrossRef]
12. Wenzel, T.J. *Differentiations of Chiral Compounds Using NMR Spectroscopy*, 2nd ed.; John Wiley & Sons: Hoboken, NJ, USA, 2018; ISBN 978-1-119-32391-4.
13. Aroulanda, C.; Lesot, P. Molecular enantiodiscrimination by NMR spectroscopy in chiral oriented systems: Concept, tools, and applications. *Chirality* **2022**, *34*, 182–244. [CrossRef]
14. Lesot, P.; Gil, R.R. Anisotropic One-dimensional/Two-dimensional NMR in Molecular Analysis: Contributions and Opportunities of Anisotropic One-dimensional/Two-dimensional NMR to Recent Analysis of Small Organic Molecules. In *Two-Dimensional (2D) NMR Methods*; Ivanov, K., Madhu, P.K., Rajalakshmi, G., Eds.; John Wiley & Sons, Ltd.: Hoboken, NJ, USA, 2023; Chapter 9; pp. 209–296. [CrossRef]
15. Beckwith, A.L.J. Synthesis of Amides. In *The Chemistry of Amides*; Zabicky, J., Ed.; Interscience: New York, NY, USA, 1970; pp. 73–185, ISBN 9780471980490.
16. Koketsu, M.; Ishihara, H. Thioureas and selenoureas and their applications. *Curr. Org. Synth.* **2006**, *3*, 439–455. [CrossRef]
17. Fenouillot, F.; Alain, R.; Colomines, G.; Sain Loup, R.; Pascault, J.P. Polymers from renewable 1,4:3,6-dianhydrohexitols (isosorbides, isomannide and isoidide): A review. *Prog. Polym. Sci.* **2010**, *35*, 578–622. [CrossRef]
18. Koert, U. *Encyclopedia of Reagents for Organic Synthesis*; John Wiley & Sons: Chichester, UK, 2012; pp. 1–5, ISBN 978-0-470-01754-8.
19. Shou, Q.; Yuan, R.; Ma, G.; Liang, X.; Wan, J.; Xian, M.; Wang, Q. Chiral nanostructures of isosorbide- and isomannide-based polyurethanes. *Polymer* **2019**, *164*, 118–125. [CrossRef]
20. Kadraoui, M.; Maunoury, T.; Derriche, Z.; Guillarme, S.; Saluzzo, C. Isohexides as Versatile Scaffolds for Asymmetric Catalysis. *Eur. J. Org. Chem.* **2015**, *2015*, 441–457. [CrossRef]
21. Chen, L.Y.; Guillarme, S.; Saluzzo, C. Dianhydrohexitols: New Tools for Organocatalysis. Application in Enantioselective FriedelCrafts Alkylation of Indoles with Nitroalkenes. *Arkivoc* **2013**, *2013*, 227–244. [CrossRef]
22. Balzano, F.; Iuliano, A.; Uccello-Barretta, G.; Zullo, V. Renewable resources for enantiodiscrimination: Chiral solvating agents for NMR spectroscopy form isomannide and isosorbide. *J. Org. Chem.* **2022**, *87*, 12698–12709. [CrossRef]
23. Zullo, V.; Gorécki, M.; Guazzelli, L.; Mezzetta, A.; Pescitelli, G.; Iuliano, A. Exploiting isohexide scaffolds for the preparation of chiral ionic liquid tweezers. *J. Mol. Liq.* **2021**, *322*, 114528. [CrossRef]
24. Iwaniuk, D.P.; Wolf, C. A versatile and practical solvating agent for enantioselective recognition and NMR analysis of protected amines. *J. Org. Chem.* **2010**, *75*, 6724–6727. [CrossRef]
25. Jain, N.; Khanvilkar, A.N.; Sahoo, S.; Bedekar, A.V. Modification of Kagan's amide for improved activity as Chiral Solvating Agent in enantiodiscrimination during NMR analysis. *Tetrahedron* **2018**, *74*, 68–76. [CrossRef]
26. Peña, C.; Gonzales-Sabín, J.; Alfonso, I.; Rebolledo, F.; Gotor, V. Cycloalkane-1,2-diamine derivatives as chiral solvating agents. Study of the structural variables controlling the NMR enantiodiscrimination of chiral carboxylic acids. *Tetrahedron* **2008**, *64*, 7709–7717. [CrossRef]
27. Yang, X.; Wang, G.; Zhong, C.; Wu, X.; Fu, E. Novel NMR chiral solvating agents derived from (1*R*,2*R*)-diaminocyclohexane: Synthesis and enantiodiscrimination for chiral carboxylic acids. *Tetrahedron Asymmetry* **2006**, *17*, 916–921. [CrossRef]
28. Ema, T.; Yamasaki, T.; Watanabe, S.; Hiyoshi, M.; Takaishi, K. A cross-coupling approach to an array of macrocyclic receptors functioning as chiral solvating agents. *J. Org. Chem.* **2018**, *83*, 10762–10769. [CrossRef]
29. Wen, J.; Feng, F.; Zhao, H.; Zheng, L.; Stavropoulos, P.; Ai, L.; Zhang, J. Chiral recognition of hydantoin derivatives enable by tetraaza macrocyclic chiral solvating agents using ^{1}H NMR spectroscopy. *J. Org. Chem.* **2022**, *87*, 7934–7944. [CrossRef]
30. Biang, G.; Fan, H.; Yang, S.; Yue, H.; Huang, H.; Zong, H.; Song, L. A chiral bisthiourea as chiral solvating agent for carboxylic acids in the presence of DMPA. *J. Org. Chem.* **2013**, *78*, 9137–9142. [CrossRef]
31. Biang, G.; Fan, H.; Huang, H.; Yang, S.; Zong, H.; Song, L. Highly effective configurational assignment using bisthioureas as chiral solvating agents in the presence of DABCO. *Org. Lett.* **2015**, *17*, 1369–1372. [CrossRef]
32. Biang, G.; Yang, S.; Huang, H.; Zong, H.; Song, L. A bisthiourea-based ^{1}H NMR chiral sensor for chiral discrimination of a variety of chiral compounds. *Sens. Actuators B Chem.* **2016**, *231*, 129–134. [CrossRef]
33. Dwivedi, A.M.; Bedekar, A.V. Determination of enantiodiscrimination of chiral acids and tetrahydropyrimidine derivatives by bis-thiourea derived chiral solvating agents by NMR spectroscopy. *Tetrahedron* **2023**, *131*, 133501. [CrossRef]
34. Gunal, S.R.; Tuncel, S.T.; Dogan, I. Enantiodiscrimination of carboxylic acids using single enantiomer thioureas as chiral solvating agents. *Tetrahedron* **2020**, *76*, 131141. [CrossRef]
35. Hernandesz-Rodrigez, M.; Juaristi, E. Structurally simple chiral thioureas as chiral solvating agents in the enantiodiscrimination of α-hydroxy and α-amino carboxylic acids. *Tetrahedron* **2008**, *63*, 7673–7678. [CrossRef]
36. Recchimurzo, A.; Micheletti, C.; Uccello-Barretta, G.; Balzano, F. Thiourea derivative of 2-[(1*R*)-1-aminoethyl]phenol: A flexible pocket-like chiral solvating agent (CSA) for the enantiodifferentiation of amino acid derivatives by NMR spectroscopy. *J. Org. Chem.* **2020**, *85*, 5342–5350. [CrossRef] [PubMed]
37. Recchimurzo, A.; Micheletti, C.; Uccello-Barretta, G.; Balzano, F. A dimeric thiourea CSA for the enantiodiscrimination of amino acid derivatives by NMR spectroscopy. *J. Org. Chem.* **2021**, *86*, 7381–7389. [CrossRef]
38. Recchimurzo, A.; Balzano, F.; Uccello-Barretta, G.; Gherardi, L. Bis-thiourea chiral sensor for the NMR enantiodiscrimination of *N*-acetyl and *N*-trifluoroacetyl amino acid derivatives. *J. Org. Chem.* **2022**, *87*, 11968–11978. [CrossRef] [PubMed]

39. De Coster, G.; Vandyck, K.; Van der Eychen, E.; Van der Eychen, J.; Elseviers, M.; Röper, H. D-isomannide in synthesis: Asymmetric Diels-Alder reactions with novel homochiral bis-imine Cu^{2+}-catalyst. *Tetrahedron Asymmetry* **2002**, *13*, 1673–1679. [CrossRef]
40. Khanh-Duy, H.; Houssein, I.; Martial, T.; Giang, V.T. New class of chiral ligands derived from isosorbide: First application in asymmetric transfer hydrogenation. *Tetrahedron Asymmetry* **2010**, *21*, 1542–1548. [CrossRef]
41. Mishra, S.K.; Suryaprakash, N. Some new protocols for the assignment of absolute configuration by NMR spectroscopy using chiral solvating agents and CDAs. *Tetrahedron Asymmetry* **2017**, *28*, 1220–1232. [CrossRef]
42. Arya, N.; Mishra, S.K.; Suryaprakash, N. A simple ternary ion-pair complexation protocol for testing the enantiopurity and the absolute configurational analysis of acid and ester derivatives. *New J. Chem.* **2018**, *42*, 9920–9929. [CrossRef]
43. Chen, Z.; Fan, H.; Yang, S.; Bian, B.; Song, L. Chiral sensors for determining the absolute configuration of α-amino acids derivatives. *Org. Biomol. Chem.* **2018**, *16*, 6933–6939. [CrossRef] [PubMed]
44. Mosher, W.A.; Heindel, N.D. Configuration assignments in symmetrical alkyl-alkyl pinacols. *J. Org. Chem.* **1963**, *28*, 2154–2155. [CrossRef]
45. Govil, G.; Hosur, R.V. *Conformation of Biological Molecules: New Result from NMR*; Springer: Berlin/Heidelberg, Germany; New York, NY, USA, 1982; pp. 18–19, ISBN 3-540-10769-X.
46. Wu, J.; Eduard, P.; Thiyagaraian, S.; Havaren, J.V.; Es, D.S.V.; Koning, C.E.; Lutz, M.; Guerra, C.F. Isohexide derivatives form renewable resources as chiral building blocks. *ChemSusChem* **2011**, *4*, 599–603. [CrossRef]
47. La Scala, J.J.; Yandek, G.; Sadler, J.M. The effect of methyl and methoxy substituents on dianilines for a thermosetting polyimide system. *High Perform. Polym.* **2020**, *32*, 801–822. [CrossRef]
48. Barros, T.G.; Pinheiro, S.; Williamson, J.S.; Tanuri, A.; Gomes, M., Jr.; Pereira, H.S.; Brindeiro, R.M.; Neto, J.B.A.; Antunes, O.A.C.; Muri, E.M.F. Pseudo-peptides derived form isomannide: Inhibitors of serine proteases. *Amino Acids* **2010**, *38*, 701–709. [CrossRef]
49. Archibald, T.G.; Baum, K. Synthesis of polynitro-2,6-dioxabicyclo[3.3.0.]octanes. *Synth. Commun.* **1989**, *19*, 1493–1498. [CrossRef]
50. Naturale, G.; Lamblin, M.; Commandeur, C.; Felpin, F.X.; Dessolin, J. Direct C-H alkylation of naphthoquinones with amino acids through a rivisited Kochi-Anderson radical decarboxylation: Trend and reactivity and application. *Eur. J. Org. Chem.* **2012**, *29*, 5774–5788. [CrossRef]
51. Natanael, J.G.; Ancock, A.H.; Wille, U. Reaction of amino acids, di- and tripeptides with the environmental oxidant NO3-: A laser flash photolysis and computational study. *Chem. Asian J.* **2016**, *11*, 3188–3195. [CrossRef] [PubMed]

Disclaimer/Publisher's Note: The statements, opinions and data contained in all publications are solely those of the individual author(s) and contributor(s) and not of MDPI and/or the editor(s). MDPI and/or the editor(s) disclaim responsibility for any injury to people or property resulting from any ideas, methods, instructions or products referred to in the content.